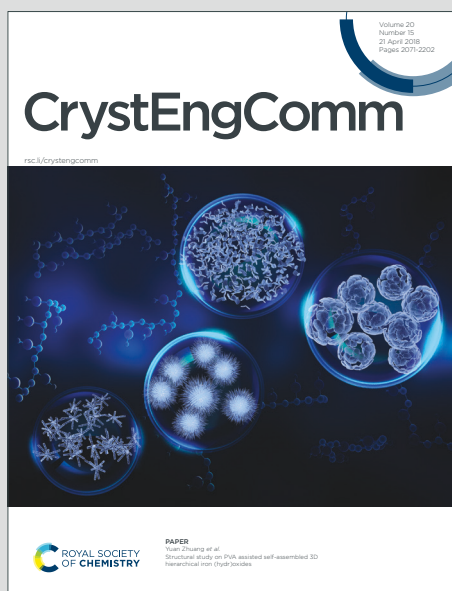


CrystEngComm

Accepted Manuscript

This article can be cited before page numbers have been issued, to do this please use: K. Kravets, M. Kravets and O. Danylyuk, *CrystEngComm*, 2025, DOI: 10.1039/D5CE00666J.



This is an Accepted Manuscript, which has been through the Royal Society of Chemistry peer review process and has been accepted for publication.

Accepted Manuscripts are published online shortly after acceptance, before technical editing, formatting and proof reading. Using this free service, authors can make their results available to the community, in citable form, before we publish the edited article. We will replace this Accepted Manuscript with the edited and formatted Advance Article as soon as it is available.

You can find more information about Accepted Manuscripts in the [Information for Authors](#).

Please note that technical editing may introduce minor changes to the text and/or graphics, which may alter content. The journal's standard [Terms & Conditions](#) and the [Ethical guidelines](#) still apply. In no event shall the Royal Society of Chemistry be held responsible for any errors or omissions in this Accepted Manuscript or any consequences arising from the use of any information it contains.

ARTICLE

Host-guest conformational adaptation in the crystal complexes of pentamidine and *p*-sulfonato-calix[*n*]arenesKateryna Kravets,^a Mykola Kravets^a and Oksana Danylyuk^{*a}Received 00th January 20xx,
Accepted 00th January 20xx

DOI: 10.1039/x0xx00000x

The structural features of the host-guest crystal complexes of *p*-sulfonato-calix[*n*]arene series (**C4S**, **C6S** and **C8S**) with pentamidine are discussed. Smaller **C4S** and **C6S** provide their outer surface as a scaffold for exclusion complexation of pentamidine guests in the C-shaped conformation fitted to the curvature of the macrocycles, while their cavities are taken by solvent molecules. The largest **C8S** flattens into distorted pleated loop conformation with pentamidine guests taking advantage of whole macrocyclic surface. The central hole of the **C8S** distorted pleated loop is available to alcohol solvent molecule, which does not interfere with the complexation of pentamidine. The host-guest complexation is also evident in the methanolic solution *via* ¹H NMR experiments, with more pronounced effect of the largest **C8S** macrocyclic host.

Introduction

p-Sulfonato-calix[*n*]arenes are popular macrocyclic compounds for (bio)molecular recognition and integration into various supramolecular systems.^{1,2} Their great advantages are high water solubility, biocompatibility and availability in the range of sizes defining cavity volumes and conformational properties of the macrocyclic skeletons. The smallest family member *p*-sulfonato-calix[4]arene **C4S** of the bowl-shaped cavity is well-known to attract metal ions and organic cations in the proximity of the anionic sulfonate rim.^{3,4,5} The π -rich aromatic cavity can contain guest molecules and ions, as well as water molecule(s).^{6,7} The typical cone conformation of **C4S** is sustained by cyclic hydrogen bonding array between hydroxylic groups at the lower rim, as showcase more than 300 crystal structures in the Cambridge Structural Database incorporating **C4S** locked in the cone conformation. The interesting exception is the sole example of the 1,3-alternate conformation of **C4S** in its complex with 4,4'-bipyridine crystallized at low pH.⁸ The larger and more flexible *p*-sulfonato-calix[5]arene,^{9,10,11} *p*-sulfonato-calix[6]arene,^{12,13} *p*-sulfonato-calix[7]arene¹⁴ and *p*-sulfonato-calix[8]arene^{15,16} are able to adopt a range of conformations spanning from pleated loop to double-cavity *up-up* or *up-down* molecular shapes. The flattened pleated loop conformation of extended molecular surface is particularly important for the controlled assembly and crystallization of proteins. For instance, *p*-sulfonato-calix[8]arene **C8S** can mask different patches of cationic protein cytochrome c giving rise to three crystal forms with different symmetries and interaction patterns.^{17,18} Not only cavity inclusion is important, also surface *exo* complexation can dictate the assembly to the limiting

scenario when all protein-protein contacts in the crystal are eliminated due to large protein-calix[8]arene interfaces.¹⁹ The nonrestricted conformational flexibility of **C8S** is also suitable for displaying a mutual induced fit molecular recognition with flexible partner molecules and construction of adaptive host-guest systems.²⁰

Much progress have been achieved in the understanding of the complexation behavior of *p*-sulfonato-calix[*n*]arenes with small guest molecules, ions and even proteins.^{21,22,23} However, despite several decades of intense research, many aspects of the assembly properties and predictability of their molecular architectures are still limited (especially for larger homologues of *n* > 4). The difficulties arise from their high conformational flexibility, oligo-ionic nature, formation of higher-order complexes, competitive complexation of metal cations (counterions) and solvent molecules, among other factors. The structural studies on the **C6S** and **C8S** complexes are still scars comparing to the wealth of crystal structures available for **C4S**. It is accepted that the difference between **C4S** and larger homologues **C6S** and **C8S** is much more than a matter of size.²⁴ Therefore, we focus on the systematic investigation of the structural aspects of the series of macrocyclic hosts (**C4S**, **C6S** and **C8S**) with the same guest candidate, pentamidine, which is a World Health Organization Essential Medicine used as antiprotozoal agent to treat the human sleeping sickness caused by *Trypanosoma brucei*. Previously, we showed that pentamidine takes compact U-shaped conformation upon inclusion into the cavity of **C4S**.²⁵ Also, the supramolecular regime of **C4S**-pentamidine host-guest complexation can be changed from inclusion to exclusion by changing the complexation and crystallization media from water to water-alcohol mixtures. Here we extend our studies on other solvent systems, and larger macrocycles **C6S** and **C8S**, Fig. 1. We show that pentamidine is suitable guest molecule for all three calixarene macrocyclic hosts, however host-guest interaction

^a Institute of Physical Chemistry Polish Academy of Sciences

† Supplementary Information available: CCDC 2469726-2469730, 2482200-2482201. For ESI and crystallographic data in CIF see DOI: 10.1039/x0xx00000x



ARTICLE

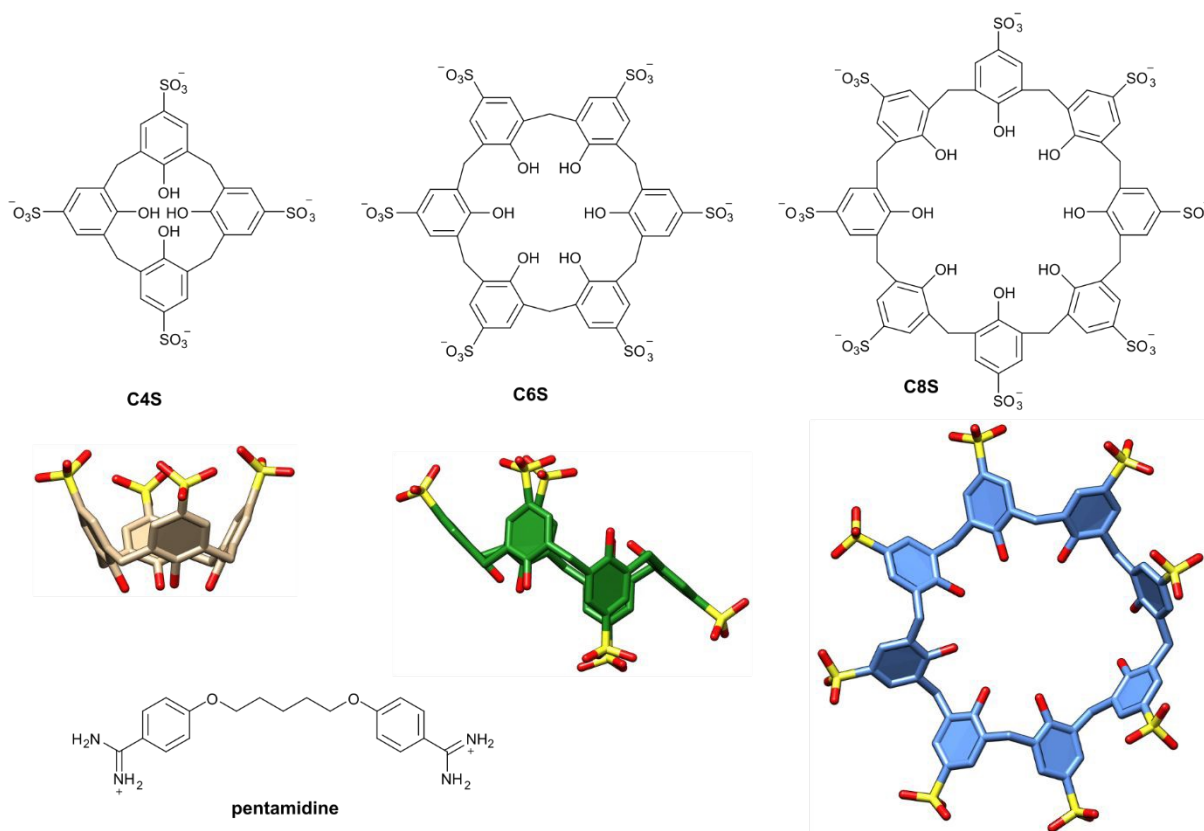


Figure 1 Molecular structures of *p*-sulfonato-calix[4]arene (**C4S**) in *cone* conformation, *p*-sulfonato-calix[6]arene (**C6S**) in the *inverted double partial cone* conformation, *p*-sulfonato-calix[8]arene (**C8S**) in the deformed *pleated loop* conformation, and pentamidine used as a guest. The drawings of the conformations for **C4S**, **C6S** and **C8S** were generated using crystal structures described in this work.

mode depends on the size of the macrocycle, as well as solvent used for the crystallization. In all mixed solvent systems **C4S** provides its outer surface as a scaffold for pentamidine molding without cavity penetration. The largest **C8S** takes distorted pleated loop shape with “*pseudo-calix[2]*” shallow cavity to hold both folded and elongated conformations of pentamidine. We discuss different scenarios of host-guest conformational adaptation in the crystal complexes, and show how solvent molecules are actively engaged in these supramolecular assemblies.

Results and discussion

The outcome of the crystallisation of **C4S** with pentamidine isethionate depends on the solvent system used to solubilise host and guest components. Our previous study showed that **C4S**-pentamidine cocrystallisation in water suffers from the rapid microprecipitation due to the effective host-guest charge neutralisation in the resulting inclusion complex, Fig. 2A.²⁵ The

addition of other solvents to water improves the solubility, but at the same time alters the interaction in the supramolecular system and structure of the final assembly. In contrast to the inclusion type complexation in aqueous media, the ¹H NMR spectrum in methanolic solution showed negligible shifts of pentamidine proton signals in the presence of **C4S**.²⁵ Following this line of study, we have attempted **C4S**-pentamidine crystallisation experiments in the mixed solvents, being successful (despite problems with microprecipitation) with water-isopropanol and water-acetone solvent mixtures. The crystallisation of **C4S** and pentamidine isethionate from water-isopropanol leads to the formation of crystalline complex **I** featuring exclusion binding of pentamidine guests to the macrocycle, Fig. 2B,C. The crystal structure was solved and refined in the monoclinic space group *P* 2₁/c. ASU consists of three crystallographically distinct **C4S** macrocycles, six pentamidines, six isopropanol and eleven water molecules. All macrocyclic cavities contain isopropanol guests hydrogen bonded to the sulfonate oxygen atoms at the upper rim, Fig.



2D,E. The inclusion of isopropanol molecules is also stabilised by C-H... π interactions between isopropanol methyl groups and aromatic subunits of **C4S**, the shortest distance between C_(methyl) and centroid of the aromatic ring is of 3.25 Å. The bowl cavity is additionally lidded by water molecule hydrogen bonded to oxygen atom of included isopropanol molecule and sulfonate oxygen of **C4S**.

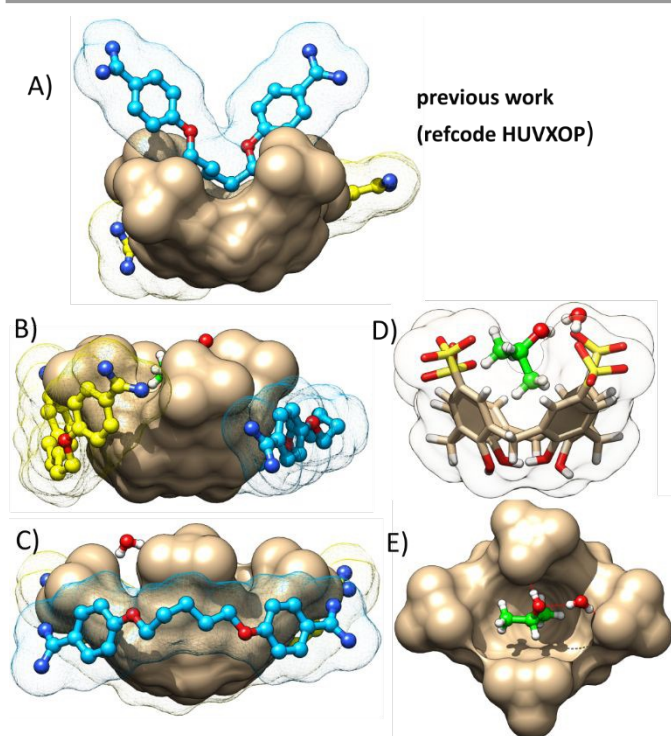


Figure 2 Host-guest complexes of **C4S** with pentamidine crystallised from (A) water, previous work, one pentamidine molecule (in blue) is included in the cavity, another (in yellow) is complexed outside; (B,C) water-isopropanol mixture, this work; two pentamidine molecules mould to the external surface of the macrocycle; (D,E) the cavity is occupied by isopropanol molecule (in green) hydrogen bonded to **C4S** upper rim. Water molecules and some hydrogen atoms omitted for clarity.

The pentamidine guests residing outside the cavities are engaged in the amidinium-sulfonate hydrogen bonding with anionic rim of **C4S**, Fig.3A. The pentamidine molecules adopt C-shaped conformation fitted to the external surface of pinched cone geometry of calix[4]arene. The distances between O...O atoms directly bound to the central aliphatic chain of pentamidine molecules are in the range of 6.0 – 6.5 Å. The curvature is less pronounced relatively to the pentamidine folded conformation (O...O distance of 4.4 Å) fixed by its inclusion into **C4S** cavity, as shown at Fig. 1A. For comparison, pentamidine can adopt an extended rod-shaped conformation (O...O distance of 7.3 Å) in its inclusion complex with carboxylated pillar[5]arene of rigid prismatic cavity accessible through two identical rims.²⁶

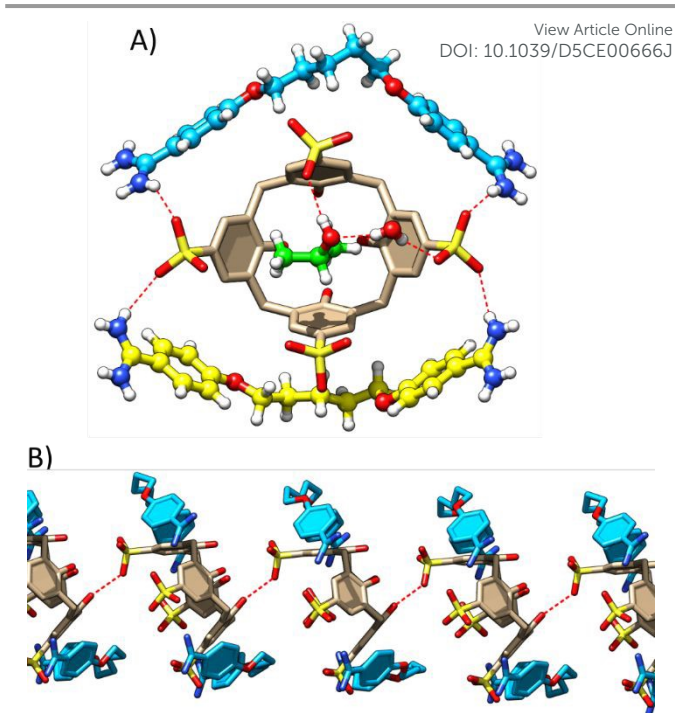


Figure 3 (A) The amidinium-sulfonate hydrogen bonding between externally complexed pentamidine molecules and **C4S** in the complex I (crystallised from water-isopropanol mixture); (B) part of the supramolecular assembly showing hydroxyl-sulfonate hydrogen bonds between adjacent **C4S** molecules in the crystal.

In the studied complex the competitive inclusion of isopropanol molecule and exclusion-type binding of pentamidine are preferable over its strong compression to fit the inner space of the bowl-shaped calix[4]arene cavity. The presence of isopropanol cosolvent as alternative guest for the cavity inclusion creates favorable conditions for the satiation of hydrophobic effect and formation of hydrogen bond between included solvent molecule and macrocyclic host. In such scenario the amidinium-sulfonate hydrogen bonding synthons between *exo* complexed pentamidine and anionic rim of **C4S** are excellently fulfilled due to snug fit between external surface of calix[4]arene and curved shape of pentamidine molecules, Fig.3A. Most of **C4S** external molecular surface is engaged in C-H... π and π ... π interactions with either pentanediol chains or benzamidine moieties of adjacent pentamidines. Almost all calix[4]arene-calix[4]arene contacts are diminished, except O-H...O hydrogen bonding between hydroxyl group at the lower rim and sulfonate oxygen atom of adjacent macrocycle, Fig. 3B. Due to the prevalence of **C4S**-pentamidine contacts engaging external surface of the macrocycles, the classical bilayer organization is perturbed in the crystal structure. Instead, the supramolecular assembly consists of **C4S** individual columns separated by pentamidine bundles, Fig. 4. The main non-covalent interactions responsible for the supramolecular architecture are C-H... π contacts between **C4S** methylene groups (as donors) and benzamidine moieties of pentamidines (as acceptors), C-H... π interactions from pentamidine pentanediol chains towards **C4S** aromatic rings, as well as some π ... π short contacts between **C4S** external surface and benzamidine moieties of pentamidine.



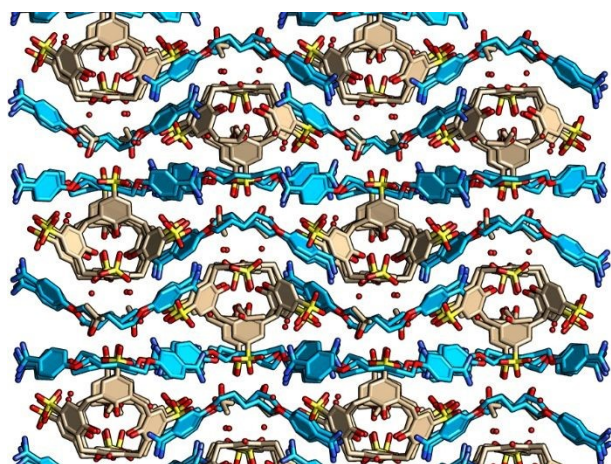


Figure 4 Crystal packing in the complex I (crystallised from water-isopropanol mixture) viewed along **b** direction; hydrogen atoms omitted for clarity; all pentamidine molecules shown in blue.

The cocrystallisation of **C4S** and pentamidine isethionate from water-acetone solvent mixture results in the formation of different crystal complex **II**, Fig. 5A,B. The crystal structure was solved and refined in the $I2/a$ monoclinic space group. The ASU contains half of the **C4S** molecule residing on the 2-fold rotation axis, one pentamidine (disordered over two positions) complexed outside of the cavity, two acetone and three water molecules. One of the acetone molecules (disordered by symmetry) fills the calix[4]arene cavity, while another resides close to the lower rim of the macrocycle, Fig. 5C,D. The exclusion complexation of pentamidine and preferential inclusion of solvent molecule are similar to the corresponding complex **I** obtained from water-isopropanol crystallization solvent. But, the mode of pentamidine molding to **C4S** external surface and amidinium-sulfonate hydrogen bonding network are different than in the complex **I**.

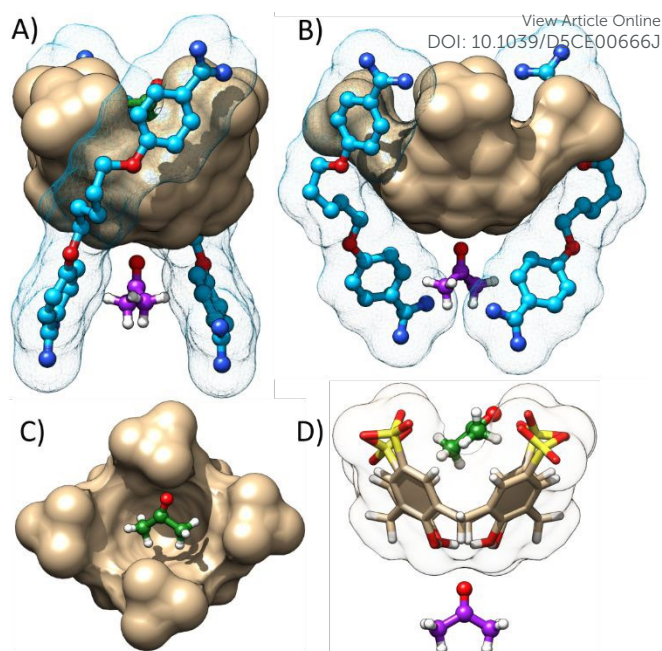


Figure 5 Host-guest complex **II** of **C4S** with pentamidine crystallised from water-acetone mixture. Water molecules and disorder omitted for clarity. (A,B) Two pentamidine molecules (in blue) mould to the external surface of the macrocycle; (C,D) the cavity is occupied by acetone molecule (in green), another acetone molecule (in violet) resides near the lower rim of the macrocycle.

The presence of additional acetone molecule at the hydrogen bonding distances to the lower rim of **C4S** is likely responsible for the change in the relative position of pentamidine guests. Due to the interaction of four lower rim hydroxyl groups with acetone molecule, the hydroxyl-sulfonate hydrogen bonding between adjacent **C4S** molecules (present in the isopropanol complex **I**) is eliminated, Fig. 6A. The pentamidine molecules interact with the sulfonate upper rim *via* one benzamidinium moiety, while another benzamidinium group is headed in the direction of lower rim to reach the sulfonate group of neighboring **C4S** macrocycle, Fig. 6B. The conformation of pentamidine guest is still C-shaped with O...O distances of 5.7 and 6.4 Å for the major and minor components of disorder, respectively. Adjacent **C4S** molecules in such supramolecular assembly are far from each other being separated by acetone and pentamidine molecules.



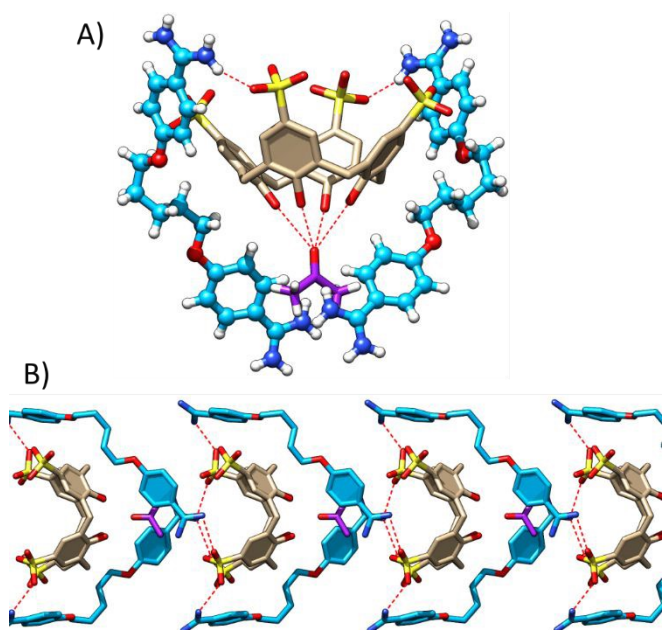


Figure 6 (A) The amidinium-sulfonate hydrogen bonding between externally complexed pentamidine molecules and **C4S**, acetone molecule near the **C4S** lower rim is at the hydrogen bonded distances with hydroxyl groups; (B) part of supramolecular assembly showing amidinium-sulfonate hydrogen bonds between pentamidines and adjacent **C4S** molecules in the crystal complex II.

The external surface of **C4S** is largely exposed to C-H... π contacts with pentamidine pentandiol chains, while calix[4]arene-calix[4]arene π ... π interactions typical for **C4S** alternative (up-down) organization are absent. As can be expected the crystal packing deviates from the well-known bilayer structural motif. Instead, the solid state assembly can be described as separated **C4S** columns connected by acetone and pentamidine molecules, Fig. 7. The overall assembly is sustained by C-H... π interactions from pentamidine pentandiol chains to **C4S** aromatic rings, while pentamidine aromatic groups are engaged in π ... π interactions with aromatic groups of adjacent pentamidine molecules in the crystal structure.

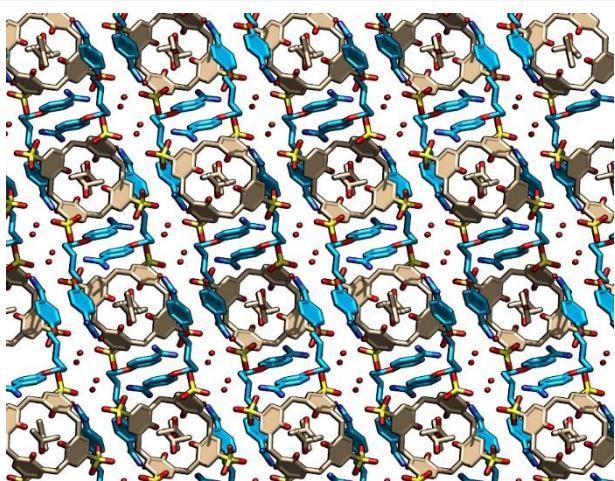


Figure 7 Crystal packing in the complex II (crystallised from water-acetone mixture) viewed along **b** direction; hydrogen atoms and disorder omitted for clarity; all pentamidine molecules shown in blue.

We have been successful to obtain **C6S**-pentamidine single crystals of sufficient diffraction quality in the case of water-methanol solvent mixture. The crystal structure of **C6S**-pentamidine complex **III** was solved and refined in the triclinic *P*-1 space group. ASU consists of one **C6S** as a hexa-anion, three pentamidine dications, two methanol and eight water molecules, Fig. 8A,B. **C6S** adopts 1,2,3-alternate conformation of compact shape featuring small inner cavity filled with methanol molecules, Fig. 8C,D. The pentamidine molecules all of similar C-shaped curvature stick to the outer surface of the macrocycle. The inner space of the calix[6]arene molecule is geometrically not available for the interaction with pentamidines. 1,2,3-Alternate conformation (also known as *up-down* or inverted double partial cone) is quite common for **C6S** host-guest complexes and assemblies,^{27,28} even in the presence of metal cations coordinated to the upper rim of the macrocycle.^{12,29} The search of CSD (version 6.00) gives 51 hits on **C6S** structures, of which 15 are isostructural **C6S** assemblies with cucurbit[8]uril in the presence of various metal ions, with **C6S** in the flattened pleated loop conformation.³⁰ Of the remaining 36 crystal structures, 28 have **C6S** in some variant of 1,2,3-alternate (*up-down* partial cone) conformation and 8 in *up-up* double cone shape. In the majority of previously described crystal structures **C6S** has two *pseudo* "calix[3]arene" cavities open in either opposite directions (*up-down*) or in the same direction (*up-up*). These partial cone cavities, albeit shallow, can accommodate various guests, as for instance crown ethers,³¹ phenanthrolines,³² amino acid L-leucine,³³ and others.³⁴

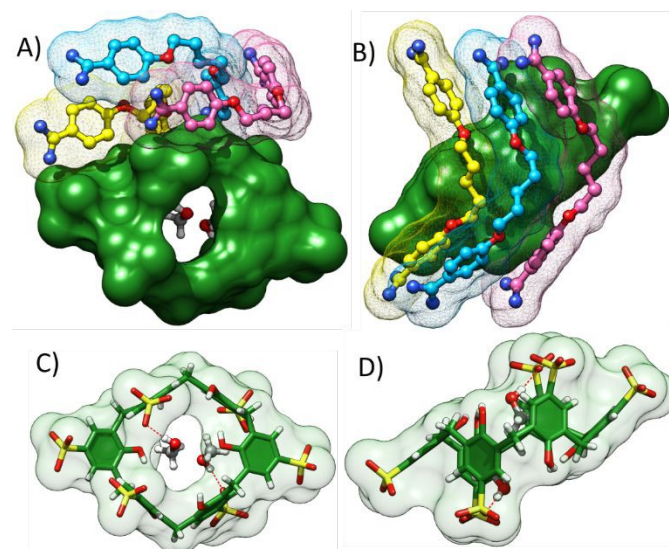


Figure 8 Host-guest complex **III** of **C6S** with pentamidine crystallised from water-methanol mixture. Water molecules and disorder omitted for clarity. (A,B) Three pentamidine molecules mould to the external surface of the macrocycle; (C,D) the cavity is occupied by two methanol molecules hydrogen bonded to sulfonate groups of the macrocycle.

Closer look at **C6S** conformation in the complex **III** reveals that both partial cones are collapsed due to inward tilting of two out of three walls framing "calix[3]arenes". Such distortion results in the complete disruption of intramolecular hydrogen bonding between OH phenolic groups usually observed in **C6S**



structures. In the **C6S**-pentamidine complex five hydroxyl groups of the macrocycle form hydrogen bonds with water molecules and one hydroxyl group interacts with sulfonate oxygen atoms of adjacent **C6S** molecules. Only small entrance to the inner space of the macrocycle remains available to let in the methanol molecules.

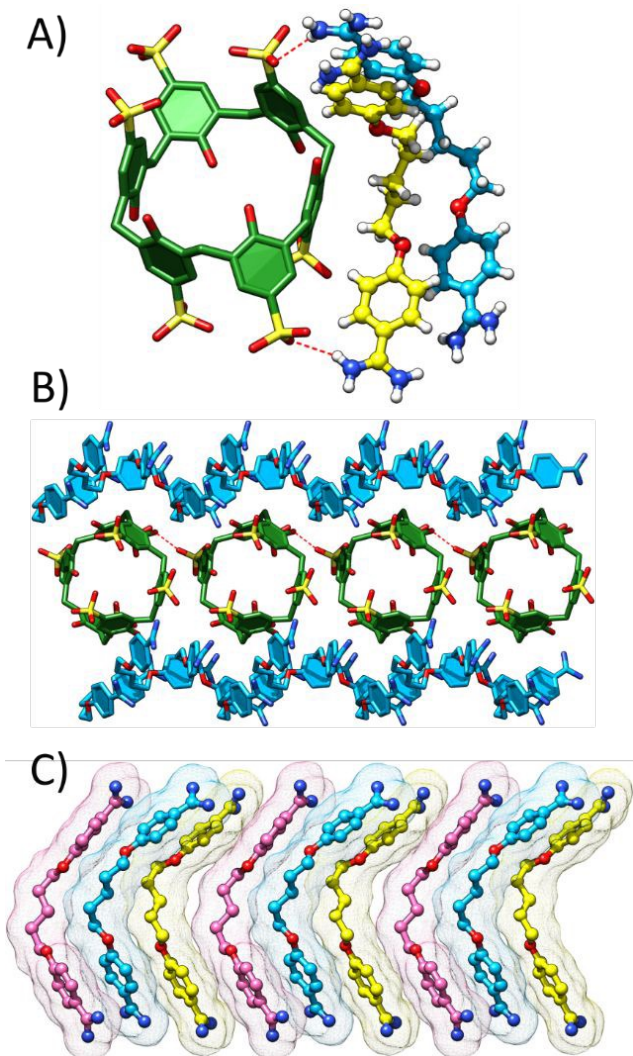


Figure 9 (A) The amidinium-sulfonate hydrogen bonding between externally complexed pentamidine molecules and **C6S** in complex III; (B) part of supramolecular assembly showing hydroxyl-sulfonate hydrogen bonds between adjacent **C6S** molecules; (C) C-shaped pentamidine molecules are in close contact with each other due to π - π stacking in the offset geometry between benzamidine moieties.

The proximity of two anionic sulfonate groups in the distorted *up-down* **C6S** conformation is compensated with their involvement in the charge-assisted hydrogen bonding with cationic amidinium donors of pentamidine molecules, Fig. 9A. Each of six sulfonate groups is engaged in this hydrogen bonding interacting with one or more amidinium groups. All three pentamidine molecules are in the C-shaped conformation fitting to the shape of each other and the external surface of the macrocycle. The distances between O...O atoms directly bound to the central aliphatic chain are in the range of 5.9 – 6.0 Å. The pentamidine conformation is again intermediate between fully extended shape observed in the case of host-guest complex

with pillar[5]arene (O...O distance of 7.3 Å)²⁶ and folded one (O...O distance of 4.4 Å) induced by pentamidine inclusion into **C4S** cavity.²⁵ The pentandiol linkers are at the C-H... π contact distances with external aromatic walls of calix[6]arene, while benzamidine aromatic moieties interact with each other *via* π - π stacking in the offset geometry, Fig. 9C. The host-guest interactions occur mainly at the anionic rim of the macrocycle as salt bridges and at the external surface of calix[6]arene, with its internal surface unavailable for pentamidine molecules. Two external aromatic walls of the macrocycle molecule participate in calix[6]arene-calix[6]arene interactions as hydroxyl-sulfonate hydrogen bonds of 2.75 Å (Fig. 9B), together with C-H... π and π - π contacts. The combination of these interactions assembles **C6S** molecules into individual rows running along *a* direction. The solid state architecture is built from separate rows of **C6S** and pentamidine molecules sewn together *via* C-H... π interactions between pentandiol linkers of pentamidines and aromatic rings of calix[4]arenes, Fig. 10. The cationic amidinium groups are clustering near sulfonate groups in the hydrophilic region of the structure. The rows of **C6S** are separated by hydrophobic bundles of pentamidine aliphatic linkers.

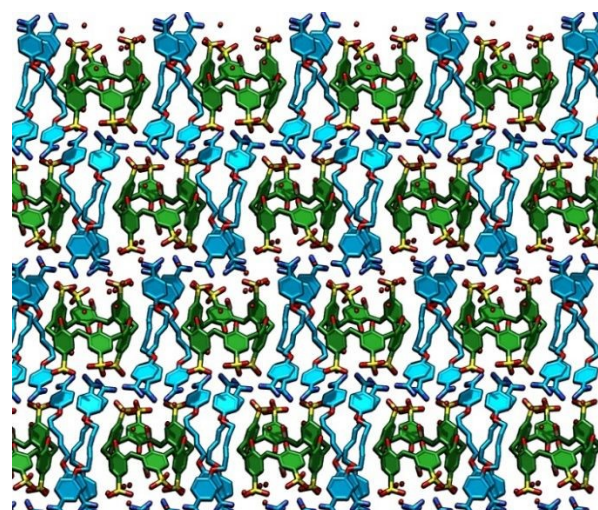


Figure 10 Crystal packing of **C6S**-pentamidine complex III (crystallized from water-methanol mixture) viewed along *a* direction; hydrogen atoms and disorder omitted for clarity; all pentamidine molecules shown in blue.

We have also looked at the host-guest complexation of pentamidine with **C6S** in CD₃OD solution using ¹H NMR spectroscopy, Fig. 11. The addition of pentamidine isethionate to **C6S** methanolic solution resulted in the rapid formation of suspension/precipitate, which partially dissolved upon gentle heating. The ¹H NMR spectra showed small shifts in the aliphatic proton signals of pentamidine (*f,g*) in the presence of **C6S**. The more pronounced upfield shifts are observed for the aromatic protons of benzamidine groups (*a,b*). The upfield shifts of all proton resonances of pentamidine suggest the inclusion host-guest complexation in the methanolic solution in contrast to the exclusion type complexes in the determined crystal structures. We previously established the inclusion possibility of benzamidine simple ligand into **C4S** cavity both in the aqueous solution and several host-guest crystal complexes.³⁵



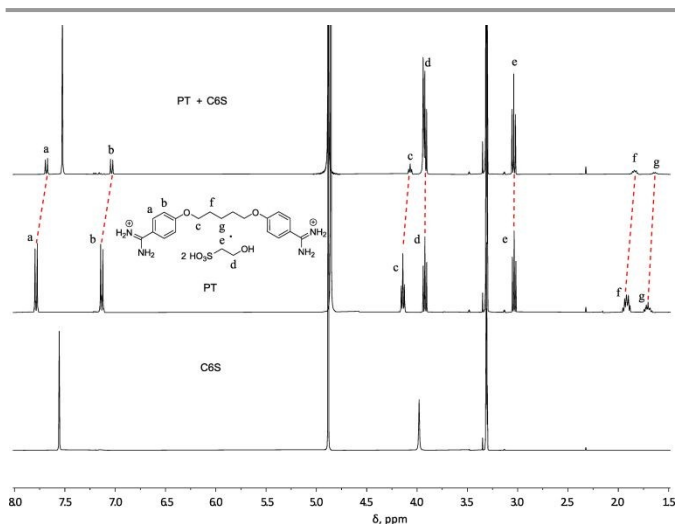


Figure 11 ^1H NMR spectra of **C6S**, pentamidine isethionate (**PT**) and host-guest complex – in the presence of slight precipitate, recorded on Agilent 400 MHz instrument at room temperature in CD_3OD . c(**C6S**) = 4 mM, c(pentamidine) = 4 mM.

The **C8S**-pentamidine cocrystallisation trials yielded single crystals in the water-ethanol and water-isopropanol solvent mixtures. Unexpectedly, the problem of microprecipitation encountered for **C4S** and **C6S** crystallisation experiments have not disturbed the crystal growth in the case of **C8S** complexes. As a result, nicely shaped prismatic crystals have been observed under the microscope next day after crystallisation set-ups, Fig. 12. Two crystal structures of complexes **IV** (obtained from water-ethanol) and **V** (from water-isopropanol mixture) appeared to be isostructural. The crystal of complex **IV** gave diffraction dataset of better quality, and this crystal structure is discussed as exemplary. The crystal structure of **C8S**-pentamidine complex **IV** was solved and refined in the monoclinic space group $C2/c$. There are two crystallographically unique **C8S** molecules of similar conformation in the asymmetric unit, besides eight pentamidines, ethanol and water molecules (disordered). The complex **IV** is highly solvated with 36.7 water molecules introduced in the structure model (38.2 water molecules for complex **V**). The implementation of SQUEEZE/PLATON³⁶ procedure on the solvent-free models to account for disordered solvent molecules as a diffuse contribution to the overall scattering resulted in improved R -values and bond precision. The final refinement results for atomistic model for the disordered solvent and alternative SQUEEZE treatment are summarized in the Experimental Section, both versions of CIF files are deposited in the CSD.

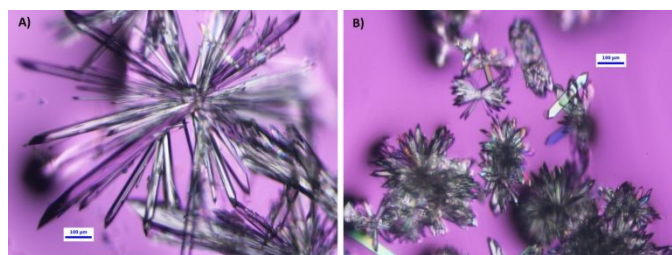


Figure 12 Photo micrographs of **C8S**-pentamidine crystal complexes obtained from water-ethanol (A) and water-isopropanol (B) solvent mixtures. Micrographs taken under polarized light.

Both calix[8]arenes adopt flattened conformation similar to the pleated loop but with two adjacent subunits in the *up-up* orientation forming *pseudo*-calix[2] shallow cavity, Fig. 13. Each **C8S** binds four pentamidine guests, two molecules on one side of the surface and two on the opposite side. While in the perfect pleated loop conformation both sides of the macrocycle are identical, here the distortion results in the de-symmetrization and distinction of two surfaces – one with *pseudo*-calix[2] cavity and two grooves, and another with three grooves, Fig. 13A,B,C. The central hole of the macrocycle is occupied by alcohol solvent molecule (ethanol in the complex **IV** and isopropanol in complex **V**) hydrogen bonded to one of the phenolic groups stabilizing the **C8S** conformation, Fig. 13D,E.

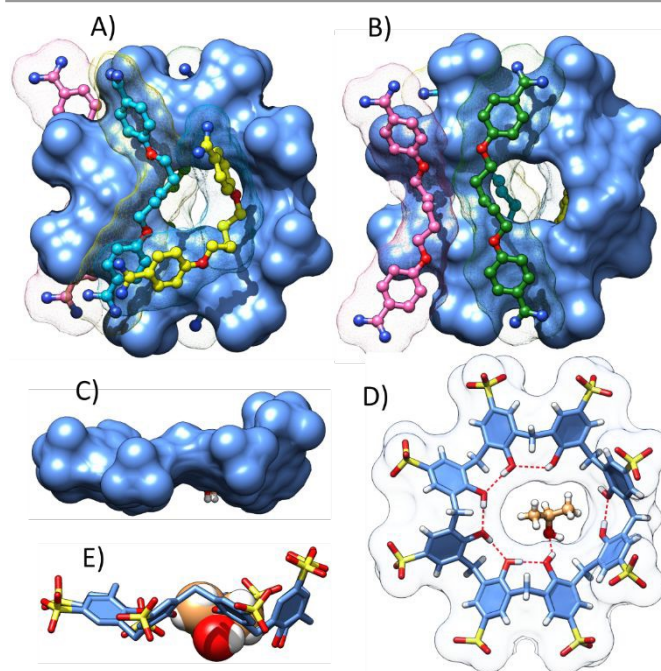


Figure 13 (A,B,C) Host-guest complex **IV** of **C8S** with pentamidine crystallised from water-ethanol mixture. Calix[8]arene molecule takes distorted pleated loop conformation with *pseudo*-calix[2] shallow cavity occupied by pentamidine in the most bend conformation (coloured in yellow), three other pentamidine molecules (coloured in blue, rose and green) fit to the grooves and bumps on the **C8S** surface. The central hole of the macrocycle holds one ethanol molecule (not shown for clarity). (D,E) the central hole in the isostructural complex **V** is occupied by isopropanol molecule hydrogen bonded to one of the hydroxyl groups of calix[8]arene. Water molecules and disorder omitted for clarity.

In the true pleated loop conformation eight hydroxyl groups are arranged in the almost planar hydrogen bonded cyclic array as shown at Fig. 14A.³⁷ The plane defined by eight coplanar oxygen atoms showcases four identical grooves (on either side of the macrocycle) generated by the kinking of the methylene bridging groups alternatively above and below this virtual plane, Fig. 14C. In the discussed host-guest complex **IV** the intramolecular hydrogen bonded array is disrupted, Fig. 14B. In this **C8S** conformation six aryl rings follow a continuous “pleated ribbon” shape sustained by five intramolecular hydrogen bonds. The deformation can be described as upright placement of two contiguous aryl moieties (*pseudo*-calix[2]) relatively to the plane defined by six oxygen atoms of the “pleated loop” part of the molecule, Fig. 14D. The methylene carbon atom bridging these



two aryl rings is coplanar with six oxygen atoms, while two hydrogen bonded hydroxyl groups within *pseudo*-calix[2] deformation project below this virtual plane. For comparison, none of the 23 crystal structures of different **C8S** assemblies deposited in the Cambridge Structural Database shows the same distorted pleated loop shape. In the previously reported host-guest, coordination and metallo-supramolecular structures of **C8S**, the macrocycle shows wide span of conformations between extreme inverted double cone (also known as *up-down* double cone) and flattened pleated loop shapes.^{38,39,40,41} **C8S** molecule can adopt unusual conformation as a combination of *pseudo* “calix[3]arene” cavity and pleated loop in the presence of tetraphenylphosphonium and aquated ytterbium(III) ions.⁴² The unrestricted conformational flexibility of the macrocyclic skeleton has been well recognized also in *p-tert*-butyl-calix[8]arene coordination complexes⁴³ and solvate structures.⁴⁴

The similar conformational fixing of pentamidine molecule is observed upon its inclusion into **C4S** cavity, as shown at Fig. 2A. Neither of the pentamidine molecules is in the fully elongated conformation, as in three crystal forms of the host-guest inclusion complex with carboxylated pillar[5]arene.²⁶ The inclusion of pentamidine into larger pillar[6]arene also does not hamper its elongated shape as macrocycle is able to squeeze around the rod-like guest to maximize the host-guest interactions.⁴⁵ Two reported and deposited in the CSD crystal structures of pentamidine isethionate salts comprise pentamidine in the elongated shape.^{46,47} In all these structures the torsional angles of the extended pentanediol linker are close to 180.0° typical for the energetically preferred *anti* conformation. The central chain torsion angles of all pentamidine molecules in the **C8S** host-guest ensemble are distorted, exemplary angles are of -78°, 72° and 83°. The crumpled conformation of the central linkers causes overall shortening of pentamidine molecules and better fitting to the curved surface of the macrocycle, enabling C-H... π , cation... π , and hydrogen bonding possibilities with **C8S**. The most elongated pentamidine molecule interacts *via* amidinium-sulfonate hydrogen bonding with sulfonate groups on the opposite edges of the pleated loop part of the macrocycle, Fig. 15A. The most folded pentamidine shows C-H... π and C-H...O close contacts of its pentanediol chain in the “*pseudo*-calix[2]” spot of the **C8S** surface, while its benzamidinium moieties point away towards adjacent **C8S** molecules in the crystal structure. Overall, the **C8S**-pentamidine ensemble can be considered as a mutually induced fit structure as both highly flexible host and guest molecules adapt their geometry for the optimal complexation.

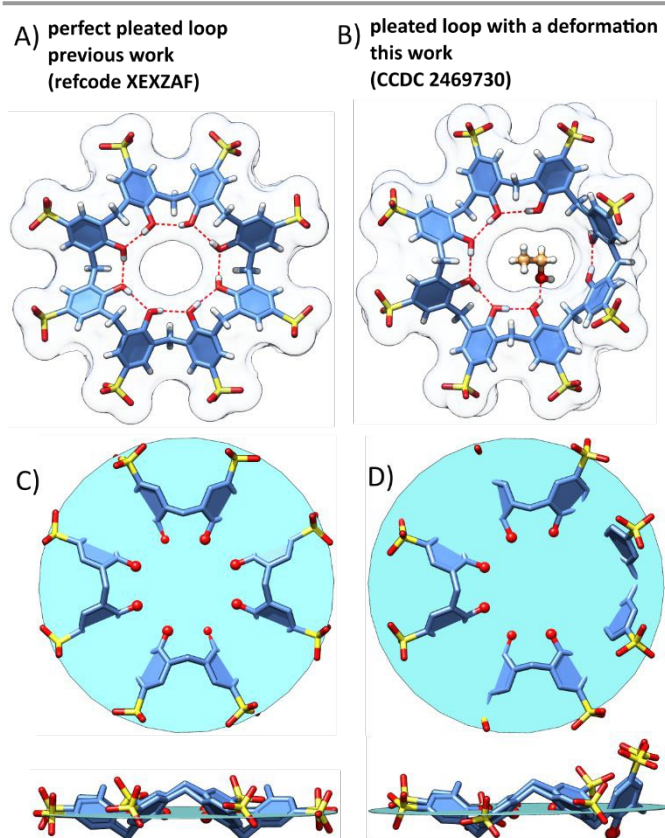


Figure 14 (A) The perfect pleated loop conformation of **C8S** of circular hydrogen bonding array at the lower rim, previous work (refcode XEXZAF). (B) The deformed pleated loop conformation of **C8S** in its host-guest complex **V** with pentamidine, circularity of hydrogen bonding is disrupted, this work. (C) In the true pleated loop molecular shape all eight hydroxyl oxygen atoms are coplanar, the virtual plane defined by eight oxygen atoms shown in blue colour. (D) In the deformed pleated loop conformation only six of eight oxygen atoms are coplanar, remaining two hydroxyl groups are positioned below the plane due to the upright orientation of two juxtaposed aryl rings.

All pentamidines are of various degree of bending adjusting to the bumps, hollows and their combination at which guests reside. The most defined curvature on the **C8S** surface is of “*pseudo*-calix[2]” shape capable of distinct U-shape guest folding (pentamidine molecule coloured in yellow at Fig. 13A).

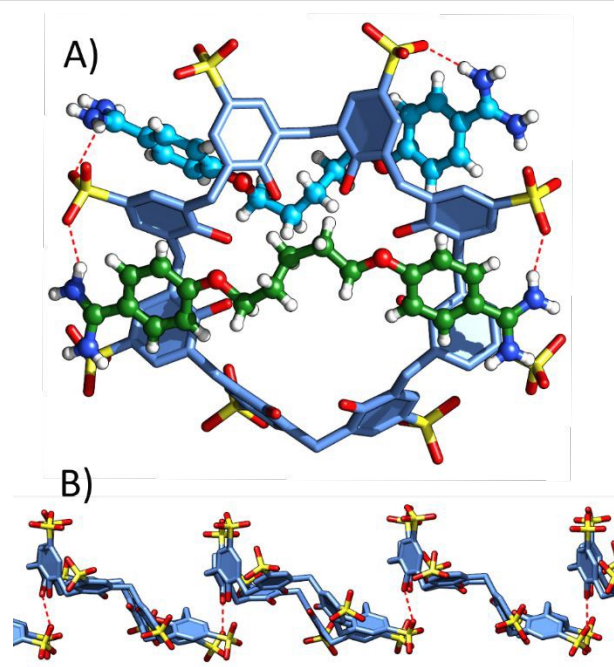


Figure 15 (A) The amidinium-sulfonate hydrogen bonding between selected pentamidine molecules and sulfonate groups in the pleated loop part of calix[8]arene in complex **IV**;



(B) intermolecular hydroxyl-sulfonate hydrogen bonding between adjacent **C8S** molecules.

The majority of the **C8S** surface is engaged in the various contacts with guest molecules. Even the external surface of the “pseudo-calix[2]” bump is covered by adjacent pentamidine. The sole interaction between neighboring **C8S** molecules in the crystal is hydroxyl-sulfonate hydrogen bonding (O-H...O distances are 2.59 and 2.70 Å), as shown at Fig. 15B. Besides this hydrogen bonding, there is no possibility for the **C8S** oligomerization through surface wall interactions. All **C8S** molecules are well separated from each other by thick bundles of pentamidines shown in yellow color at Fig. 16. The supramolecular architecture is supported by multiple **C8S**-pentamidine interactions, these include $\pi\cdots\pi$ contacts in face-to-face and edge-to-face orientation between **C8S** aromatic rings and pentamidine benzamidine groups, C-H... π interactions from macrocycle methylene groups towards pentamidine aromatic moieties, and C-H... π interactions from pentamidine pentanediol chains to calix[8]arene aromatic rings. Additionally, $\pi\cdots\pi$ and C-H... π interactions between adjacent pentamidine molecules can be identified within their bundles. Multiple water molecules in the interconnected channels take *app.* 20 % of the crystal volume. In the previously reported **C8S** sodium salts structures the stacking of adjacent macrocycles is efficiently realized through pleated loop surface interactions and coordination of metal cation.^{37,48} Also, **C8S** can oligomerize into dimeric or trimeric macrocycle supramolecular synthons in the crystal structures with selected proteins.^{49,50}

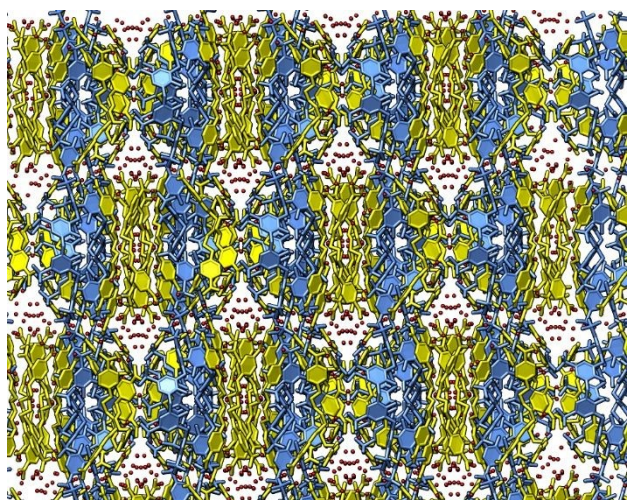


Figure 16 Crystal packing of **C8S**-pentamidine complex **IV**; hydrogen atoms and disorder omitted for clarity; all pentamidine molecules shown in yellow colour, all **C8S** molecules are in cornflower blue colour.

The host-guest complexation between pentamidine and **C8S** in CD₃OD solution was confirmed by ¹H NMR spectroscopy, Fig. 17. Upon mixing **C8S** and pentamidine solutions, a slight precipitate formed, which partially dissolved upon gentle heating. The ¹H NMR spectra showed minor shifts of the aliphatic proton signals of pentamidine (f,g) in the presence of **C8S**. Large upfield shifts are visible for the aromatic protons of benzamidine groups (a,b), even more pronounced compared

to the shifts observed in the case of **C6S**-pentamidine complex. Such large shifts of aromatic proton resonances indicate deep inclusion of the guest benzamidine groups into the host cavity. Thus, it might be expected that **C8S** molecule takes more globular shape of substantial cavity in the solution relatively to the flattened pleated loop conformation observed in the crystal complex.

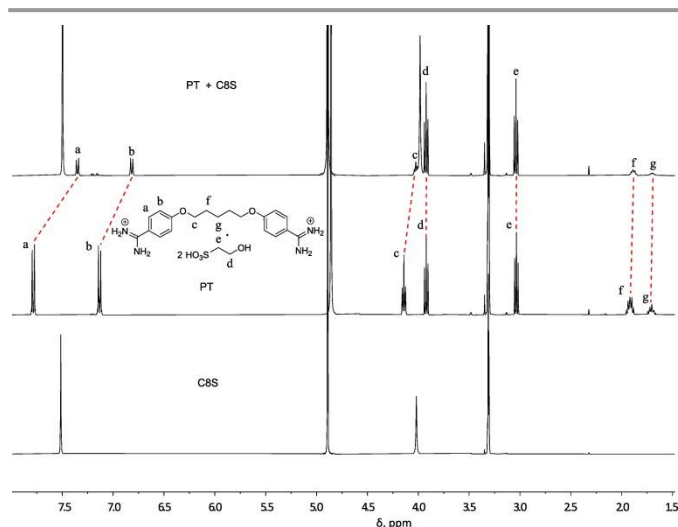


Figure 17 ¹H NMR spectra of **C8S**, pentamidine isethionate (**PT**) and host-guest complex – in the presence of slight precipitate, recorded on Agilent 400 MHz instrument at room temperature in CD₃OD. c(**C8S**) = 4 mM, c(pentamidine) = 4 mM.

Conclusions

Host-guest crystal complexes between *p*-sulfonato-calix[*n*]arenes and pentamidine show high degree of structural and supramolecular adaptation in terms of induced fit, mutual induced fit and competitive/cooperative inclusion of solvent molecules. The calix[*n*]arene-pentamidine interactions are efficiently realized not only in the classical inclusion mode requiring pentamidine folding into compact U-shape,²⁵ but also through *exo*-wall surface interactions involving pentamidine C-shaped gentler bending. Pentamidine molecules in the C-shaped conformation mould closely to the outer surface curvature of **C4S** and **C6S** while forming amidinium-sulfonate hydrogen bonding by two terminal benzamidine moieties. Indeed, pentamidine as a guest is able to significantly perturb common bilayer arrangement of **C4S** and **C6S** molecules usually realized through a combination of $\pi\cdots\pi$ and C-H... π interactions between external walls of adjacent macrocycles. The disruption of calixarene-calixarene contacts and consequently bilayer organisation reminds the pentamidine well-known ability to disorder the *quasi*-crystalline structure of the LPS monolayer on the bacteria outer membrane.⁵¹

The largest **C8S** molecule flattens into distorted pleated loop conformation with pentamidine guests taking advantage of whole macrocyclic surface. In this conformation the differentiation between inner and outer surface is blurred, as the **C8S** shape evolved towards a solid torus like structure (with a deformation) in comparison to cone shape of the smallest homologue **C4S**. The central hole of the **C8S** distorted pleated



loop is available to alcohol solvent molecule. Again, in this crystal complex all calixarene-calixarene contacts are diminished (except scarce hydroxyl-sulfonate hydrogen bonding) due to rich **C4S**-pentamidine interactions. Potentially, the portfolio of the possible conformations for **C8S** can be further expanded pursuing the cocrystallisation and structural characterisation of its complexes and assemblies. These can benefit the growing application of macrocycles as tectons in directing protein assembly and crystal engineering.⁵²

Experimental

Pentamidine isethionate, *p*-sulfonato-calix[4]arene, *p*-sulfonato-calix[6]arene and *p*-sulfonato-calix[8]arene were purchased from TCI Europe and used as received. ¹H NMR spectra were recorded on an Agilent 400 MHz instrument using CD₃OD solvent at room temperature.

Crystallisation conditions

Complex I: 5 mg of **C4S** was dissolved in 0.5 ml of 1:1 water-isopropanol mixture. The solution of 4.6 mg of pentamidine isethionate in 0.5 ml of 1:1 water-isopropanol mixture was slowly added to the solution of **C4S**. The clouding of the solution was observed followed by some microprecipitation. Prismatic shaped crystals of complex **I** suitable for diffraction were found after several days.

Complex II: 5 mg of **C4S** was dissolved in 0.5 ml of 1:1 water-acetone mixture. The solution of 4.6 mg of pentamidine isethionate in 0.5 ml of 1:1 water-acetone mixture was slowly added to the solution of **C4S**. Rapid clouding of the solution was observed followed by microprecipitation. Plate-like crystals of complex **II** suitable for diffraction were found within the precipitate after several days.

Complex III: 20 mg of **C6S** was dissolved in 0.5 ml of 1:1 water-methanol mixture. The solution of 18.3 mg of pentamidine isethionate in 0.5 ml of 1:1 water-methanol mixture was slowly added to the solution of **C6S**. Rapid clouding of the solution was observed followed by microprecipitation. Prismatic crystals of complex **III** suitable for diffraction were found within the precipitate after 10 days.

Complex IV: 20 mg of **C8S** was dissolved in 1 ml of 1:1 water-ethanol mixture. The solution of 9.1 mg of pentamidine isethionate in 1 ml of 1:1 water-ethanol mixture was slowly added to the solution of **C8S**. The clouding of the solution was observed. Prismatic crystals of complex **IV** suitable for diffraction were found the next day.

Complex V: 20 mg of **C8S** was dissolved in 1 ml of 1:1 water-isopropanol mixture. The solution of 9.1 mg of pentamidine isethionate in 1 ml of 1:1 water-isopropanol mixture was slowly added to the solution of **C8S**. The clouding of the solution was observed. Prismatic crystals of complex **V** suitable for diffraction were found the next day.

Crystallography

The crystals were embedded in the inert perfluoropolyalkylether (viscosity 1800cSt; ABCR GmbH) and mounted using Hampton Research Cryoloops. The crystals were

flash cooled to 100.0(1) K in a nitrogen gas stream and kept at this temperature during the experiments. The X-ray data were collected on a SuperNova Agilent diffractometer using CuK α radiation ($\lambda = 1.54184$ Å). The data were processed with *CrysAlis PRO* software. Structures were solved by direct methods and refined using *SHELXL*⁵³ under *WinGX*.⁵⁴ The crystal complexes **IV** and **V** are highly solvated with many disordered water molecules introduced in the structure models. Alternatively, to address the solvent disorder issue the SQUEEZE/PLATON method³⁶ was implemented on **IV** and **V**. The contribution of disordered water molecules removed by SQUEEZE have been included in the overall formula, formula weight, density, etc. The refinement details for complexes **IV** and **V** with and without SQUEEZE are given below. The figures were prepared using *Chimera*.⁵⁵

Crystal data for complex I: $3(\text{C}_{28}\text{H}_{20}\text{O}_{16}\text{S}_4) \cdot 6(\text{C}_{19}\text{H}_{26}\text{N}_4\text{O}_2) \cdot 6(\text{C}_3\text{H}_8\text{O}) \cdot 11(\text{H}_2\text{O})$, $M_r = 4835.4$, colourless prisms, monoclinic, space group $P 2_1/c$, $a = 23.6106(1)$, $b = 30.3731(2)$, $c = 31.5092(2)$ Å, $\beta = 91.424(1)^\circ$, $V = 22589.1(2)$ Å³, $Z = 4$, $\rho_{\text{calc}} = 1.42$ g·cm⁻³, $\mu(\text{CuK}\alpha) = 1.89$ mm⁻¹, $\theta_{\text{max}} = 70.1^\circ$, 145447 reflections measured, 42468 unique, 2977 parameters, $R = 0.060$, $wR = 0.162$ ($R = 0.075$, $wR = 0.174$ for all data). Goof = 1.03. CCDC 2469729.

Crystal data for complex II: $(\text{C}_{28}\text{H}_{20}\text{O}_{16}\text{S}_4) \cdot 2(\text{C}_{19}\text{H}_{26}\text{N}_4\text{O}_2) \cdot 2(\text{C}_3\text{H}_8\text{O}) \cdot 6(\text{H}_2\text{O})$, $M_r = 1649.8$, colourless plate, monoclinic, space group $I 2/a$, $a = 25.024(3)$, $b = 13.519(2)$, $c = 24.370(4)$ Å, $\beta = 108.954(17)^\circ$, $V = 7798(2)$ Å³, $Z = 4$, $\rho_{\text{calc}} = 1.41$ g·cm⁻³, $\mu(\text{CuK}\alpha) = 1.86$ mm⁻¹, $\theta_{\text{max}} = 65.1^\circ$, 44737 reflections measured, 6650 unique, 803 parameters, $R = 0.123$, $wR = 0.355$ ($R = 0.157$, $wR = 0.399$ for all data). Goof = 1.12. CCDC 2469727.

Crystal data for complex III: $(\text{C}_{42}\text{H}_{30}\text{O}_{24}\text{S}_6) \cdot 3(\text{C}_{19}\text{H}_{26}\text{N}_4\text{O}_2) \cdot 2(\text{CH}_4\text{O}) \cdot 8.3(\text{H}_2\text{O})$, $M_r = 2351.5$, colourless prisms, triclinic, space group $P -1$, $a = 12.3629(5)$, $b = 16.5072(7)$, $c = 28.5794(17)$ Å, $\alpha = 85.914(4)^\circ$, $\beta = 85.670(4)^\circ$, $\gamma = 74.715(4)^\circ$, $V = 5602.0(5)$ Å³, $Z = 2$, $\rho_{\text{calc}} = 1.39$ g·cm⁻³, $\mu(\text{CuK}\alpha) = 1.90$ mm⁻¹, $\theta_{\text{max}} = 60.9^\circ$, 31818 reflections measured, 16703 unique, 1774 parameters, $R = 0.117$, $wR = 0.310$ ($R = 0.173$, $wR = 0.350$ for all data). Goof = 1.06. CCDC 2469726.

Crystal data for complex IV: $2(\text{C}_{56}\text{H}_{40}\text{O}_{32}\text{S}_8) \cdot 8(\text{C}_{19}\text{H}_{26}\text{N}_4\text{O}_2) \cdot 2.5(\text{C}_2\text{H}_6\text{O}) \cdot 36.7(\text{H}_2\text{O})$, $M_r = 6478.8$, colourless prisms, monoclinic, space group $C 2/c$, $a = 33.9061(5)$, $b = 41.7359(5)$, $c = 46.4819(7)$ Å, $\beta = 94.332(2)^\circ$, $V = 65588.7(16)$ Å³, $Z = 8$, $\rho_{\text{calc}} = 1.31$ g·cm⁻³, $\mu(\text{CuK}\alpha) = 1.78$ mm⁻¹, $\theta_{\text{max}} = 66.6^\circ$, 637017 reflections measured, 57878 unique, 4955 parameters, $R = 0.127$, $wR = 0.325$ ($R = 0.191$, $wR = 0.394$ for all data). Goof = 1.18. CCDC 2469730.

Crystal data for complex IV_squeeze: $2(\text{C}_{56}\text{H}_{40}\text{O}_{32}\text{S}_8) \cdot 8(\text{C}_{19}\text{H}_{26}\text{N}_4\text{O}_2) \cdot 2(\text{C}_2\text{H}_6\text{O}) \cdot 48.3(\text{H}_2\text{O})$, $M_r = 6664.3$, colourless prisms, monoclinic, space group $C 2/c$, $a = 33.9061(5)$, $b = 41.7359(5)$, $c = 46.4819(7)$ Å, $\beta = 94.332(2)^\circ$, $V = 65588.7(16)$ Å³, $Z = 8$, $\rho_{\text{calc}} = 1.35$ g·cm⁻³, $\mu(\text{CuK}\alpha) = 1.82$ mm⁻¹, $\theta_{\text{max}} = 66.6^\circ$, 637017 reflections measured, 57878 unique, 4340 parameters, $R = 0.114$, $wR = 0.309$ ($R = 0.174$, $wR = 0.380$ for all data). Goof = 1.14. CCDC 2482200.

Crystal data for complex V: $2(\text{C}_{56}\text{H}_{40}\text{O}_{32}\text{S}_8) \cdot 8(\text{C}_{19}\text{H}_{26}\text{N}_4\text{O}_2) \cdot 2(\text{C}_3\text{H}_8\text{O}) \cdot 38.2(\text{H}_2\text{O})$, $M_r = 6511.3$, colourless prisms, monoclinic, space group $C 2/c$, $a = 34.1908(18)$, $b =$



41.4283(12), $c = 46.9910(18)$ Å, $\beta = 95.325(5)^\circ$, $V = 66274(5)$ Å³, $Z = 8$, $\rho_{\text{calc}} = 1.31$ g·cm⁻³, $\mu(\text{CuK}\alpha) = 1.76$ mm⁻¹, $\theta_{\text{max}} = 58.9^\circ$, 129320 reflections measured, 47500 unique, 4456 parameters, $R = 0.133$, $wR = 0.333$ ($R = 0.323$, $wR = 0.496$ for all data). Goof = 0.93. CCDC2469728.

Crystal data for complex V_squeeze: $2(\text{C}_{56}\text{H}_{40}\text{O}_{32}\text{S}_8) \cdot 8(\text{C}_{19}\text{H}_{26}\text{N}_4\text{O}_2) \cdot 2(\text{C}_3\text{H}_8\text{O}) \cdot 54(\text{H}_2\text{O})$, $M_r = 6795.3$, colourless prisms, monoclinic, space group $C 2/c$, $a = 34.1908(18)$, $b = 41.4283(12)$, $c = 46.9910(18)$ Å, $\beta = 95.325(5)^\circ$, $V = 66274(5)$ Å³, $Z = 8$, $\rho_{\text{calc}} = 1.36$ g·cm⁻³, $\mu(\text{CuK}\alpha) = 1.82$ mm⁻¹, $\theta_{\text{max}} = 58.9^\circ$, 129320 reflections measured, 47500 unique, 4049 parameters, $R = 0.119$, $wR = 0.280$ ($R = 0.289$, $wR = 0.415$ for all data). Goof = 0.92. CCDC 2482201.

Conflicts of interest

There are no conflicts to declare.

Data availability

Crystallographic data for complexes I-V have been deposited at the CCDC under numbers 2469726-2469730, for **IV_squeeze** and **V_squeeze** under numbers 2482200-2482201.

Acknowledgements

This project was funded by the National Science Centre of Poland (grant PRELUDIUM BIS no. 2019/35/O/ST4/01865).

Notes and references

¹ D.-S. Guo, Y. Liu, *Acc. Chem. Res.*, 2014, **47**, 1925.

² A.-N. Lazar, F. Perret, M. Perez-Lloret, M. Michaud, A. W. Coleman, *Eur. J. Med. Chem.*, 2024, **264**, 115994.

³ S. Shinkai, K. Araki, T. Matsuda, N. Nishiyama, H. Ikeda, I. Takasu, M. Iwamoto, *J. Am. Chem. Soc.*, 1990, **112**, 9053.

⁴ J. L. Atwood, L. J. Barbour, M. J. Hardie, C. L. Raston, *Coord. Chem. Rev.*, 2001, **222**, 3.

⁵ O. Danylyuk, K. Suwinska, *Chem Commun.*, 2009, **36**, 5799.

⁶ K. Fucke, K. M. Anderson, M. H. Filby, M. Henry, J. Wright, S. A. Mason, M. J. Gutmann, L. J. Barbour, C. Oliver, A. W. Coleman, J. L. Atwood, J. A. K. Howard, J. W. Steed, *Chem. Eur. J.*, 2011, **17**, 10259.

⁷ P. C. Leverd, P. Berthault, M. Lance, M. Nierlich, *Eur. J. Org. Chem.*, 2000, **1**, 133.

⁸ L. J. Barbour, J. L. Atwood, *Chem. Commun.*, 2001, 2020.

⁹ J. W. Steed, C. P. Johnson, C. L. Barnes, R. K. Juneja, J. L. Atwood, S. Reilly, R. L. Hollis, P. H. Smith, D. L. Clark, *J. Am. Chem. Soc.*, 1995, **117**, 11426.

¹⁰ S. J. Dalgarno, M. J. Hardie, C. L. Raston, *Chem. Commun.*, 2004, 2802.

¹¹ I. Ling, Y. Alias, B. W. Skelton, C. L. Raston, *Cryst. Growth Des.*, 2012, **12**, 1564.

¹² S. J. Dalgarno, M. J. Hardie, J. L. Atwood, C. L. Raston, *Inorg. Chem.*, 2004, **43**, 6351.

¹³ M. Makha, C. L. Raston, A. N. Sobolev, A. H. White, *Chem. Commun.*, 2005, 1962.

¹⁴ L. Erra, C. Tedesco, G. Vaughan, M. Brunelli, F. Troisi, C. Gaeta, P. Neri, *CrystEngComm*, 2010, **12**, 3463.

¹⁵ S. J. Dalgarno, M. J. Hardie, J. L. Atwood, J. E. Warren, C. L. Raston, *New J. Chem.*, 2005, **29**, 649.

¹⁶ B. Lesniewska, F. Perret, K. Suwinska, A. W. Coleman, *CrystEngComm*, 2014, **16**, 4399.

¹⁷ M. L. Rennie, G. C. Fox, J. Pérez, P. B. Crowley, *Angew. Chem. Int. Ed.*, 2018, **57**, 13764.

¹⁸ S. Engilberge, M. L. Rennie, E. Dumont, P. B. Crowley, *ACS Nano*, 2019, **13**, 10343.

¹⁹ R. J. Flood, L. Cerofolini, M. Fragai, P. B. Crowley, *Biomacromolecules*, 2024, **25**, 1303.

²⁰ A. Specht, P. Bernard, M. Goeldner, L. Peng, *Angew. Chem. Int. Ed.*, 2002, **41**, 4706.

²¹ S. J. Dalgarno, J. L. Atwood, C. L. Raston, *Chem. Commun.*, 2006, 4567.

²² I. Ling, C. L. Raston, *Coord. Chem. Rev.*, 2018, **375**, 80.

²³ P. B. Crowley, *Acc. Chem. Res.*, 2022, **55**, 2019.

²⁴ N. Lavande, A. Acuña, N. Basílio, V. Francisco, D. D. Malkhedeb, L. Garcia-Rio, *Phys. Chem. Chem. Phys.*, 2017, **19**, 13640.

²⁵ K. Kravets, M. Kravets, V. Sashuk, F. Perret, W. Maskani, D. Albertini, A.-N. Lazar, M. M. Zimnicka, O. Danylyuk, *Chem. Eur. J.*, 2025, **31**, e202404625.

²⁶ H. Butkiewicz, S. Kosior, V. Sashuk, M. Zimnicka, O. Danylyuk, *Cryst. Growth Des.*, 2022, **22**, 2854.

²⁷ Y. Liu, Q. Li, D.-S. Guo, K. Chen, *CrystEngComm*, 2008, **10**, 675.

²⁸ B. Leśniewska, A. W. Coleman, F. Perret, K. Suwinska, *Cryst. Growth Des.*, 2019, **19**, 1695.

²⁹ Y. Liu, W. Liao, Y. Bi, X. Wang, H. Zhang, *Cryst. Growth Des.*, 2009, **9**, 5311.

³⁰ L.-F. Tian, M. Liu, L.-X. Chen, C. Huang, Q.-J. Zhu, K. Chen, J.-L. Zhao, Z. Tao, *Chin. Chem. Lett.*, 2022, **33**, 1524.

³¹ S. J. Dalgarno, M. J. Hardie, M. Makha, C. L. Raston, *Chem. Eur. J.*, 2003, **9**, 2834.

³² Y. Liu, Y. Bi, W. He, X. Wang, W. Liao, H. Zhang, *J. Mol. Struct.*, 2009, **919**, 235.

³³ J. L. Atwood, S. J. Dalgarno, M. J. Hardie, C. L. Raston, *Chem.*



- Commun.*, 2005, **337**.
- ³⁴ A. N. Lazar, O. Danylyuk, K. Suwinska, R. Kassab, A. W. Coleman, *New J. Chem.*, 2008, **32**, 2116.
- ³⁵ K. Kravets, M. Kravets, O. Danylyuk, *Cryst. Growth Des.*, 2024, **24**, 10338.
- ³⁶ A. L. Spek, *Acta Crystallogr., Sect. C: Struct. Chem.* 2015, **C71**, 9.
- ³⁷ K. Kravets, M. Kravets, K. Kędra, O. Danylyuk, *Supramol. Chem.*, 2021, **33**, 666.
- ³⁸ F. Perret, V. Bonnard, O. Danylyuk, K. Suwinska, A. W. Coleman, *New J. Chem.*, 2006, **30**, 987.
- ³⁹ Y. Liu, W. Liao, Y. Bi, M. Wang, Z. Wu, X. Wang, Z. Su, H. Zhang, *CrystEngComm*, 2009, **11**, 1803.
- ⁴⁰ O. Danylyuk, H. Butkiewicz, A. W. Coleman, K. Suwinska, *J. Mol. Struct.*, 2017, **1150**, 28.
- ⁴¹ J. M. Alex, P. McArdle, P. B. Crowley, *CrystEngComm*, 2020, **22**, 14.
- ⁴² M. Makha, A. N. Sobolev, C. L. Raston, *Chem. Commun.*, 2006, 511.
- ⁴³ A. Chakraborty, L. R. B. Wilson, S. J. Dalgarno, E. K. Brechin, *Chem. Commun.*, 2025, **61**, 1104.
- ⁴⁴ A. Kieliszek, M. Malinska, *Cryst. Growth Des.*, 2021, **21**, 6862.
- ⁴⁵ H. Butkiewicz, S. Kosiorek, V. Sashuk, M. M. Zimnicka, O. Danylyuk, *Cryst. Growth Des.*, 2023, **23**, 11.
- ⁴⁶ P. R. Lowe, C. E. Sansom, C. H. Schwalbe, M. F. G. Stevens, *J. Chem. Soc., Chem. Commun.*, 1989, 1164.
- ⁴⁷ T. Srikrishnan, N. C. De, A. S. Alam, J. Kapoor, *J. Chem. Cryst.*, 2004, **34**, 813.
- ⁴⁸ R. J. Flood, N. M. Mockler, A. Thureau, M. Malinska, P. B. Crowley, *Cryst. Growth Des.*, 2024, **24**, 2149.
- ⁴⁹ K. O. Ramberg, S. Engilberge, T. Skorek, P. B. Crowley, *J. Am. Chem. Soc.*, 2021, **143**, 1896.
- ⁵⁰ N. M. Mockler, K. O. Ramberg, F. Guagnini, C. L. Raston, P. B. Crowley, *Cryst. Growth Des.*, 2021, **21**, 1424.
- ⁵¹ J. M. Stokes, C. R. Macnair, B. Ilyas, S. French, J.-P. Côté, C. Bouwman, M. A. Farha, A. O. Sieron, C. Whitfield, B. K. Coombes, E. D. Brown, *Nat. Microbiol.*, 2017, **2**, 17028.
- ⁵² N. M. Mockler, P. B. Crowley, *Biophys. Rev.*, 2025, doi.org/10.1007/s12551-025-01323-9.
- ⁵³ G. M. Sheldrick, *Acta Crystallogr. Sect. C*, 2015, **71**, 3.
- ⁵⁴ L. J. Farrugia, *J. Appl. Cryst.*, 1999, **32**, 837.
- ⁵⁵ E. F. Pettersen, T. D. Goddard, C. C. Huang, G. S. Couch, D. M. Greenblatt, E. C. Meng, T. E. Ferrin, *J. Comput. Chem.*, 2004, **25**, 1605.

